Electronic Supplementary Information

Table of Contents

1. Experimental Section

1.1. Materials

Commercially available (Alfa Aesar and Aldrich) 1,4-dibromobutane, salicylic acid, toluene, 2-butanone, chloroform, heptane, ethyl acetate, acetonitrile were used as received without further purification. Potassium carbonate was calcined before use.

1.2. Methods

Electronic absorption spectra were recorded on a Specord M-400 spectrophotometer. ^{1}H and ^{13}C NMR spectra were recorded on a Bruker Avance III spectrometer (500 and 126 MHz) with $CDCl_3$ as solvent. Chemical shifts (δ) in ppm are reported with the use of the residual chloroform signals (7.26 for ^{1}H and 77.0 for ^{13}C) as internal reference. IR spectra were performed using a Spectrum BX-2 Fourier spectrometer. The elemental analysis was measured with an Elementar vario MICRO cube analyzer. Melting points were determined on a Koffler hot stage apparatus with a heating rate of 4 °C/min.

Fluorescence studies were carried out at the Analytical Center for Collective Use tool base of the IPCP RAS: emission spectra were recorded on a PerkinElmer LS-55 spectrofluorimeter, the fluorescence decay kinetics was measured on a time-resolved FluoTime 200 fluorescence spectrometer (PicoQuant GmbH company) in the counting mode of photons GmbH. Fluorescence quantum yields (φ_{fl}) were measured using anthracene in ethanol as the standard ($\varphi_{fl} = 0.3$) [S1], with an accuracy of ±15%.

Mass spectra were recorded on a Shimadzu LC-20 Prominence gas chromatography-mass spectrometer with electrospray ionization (ESI-MS); high resolution mass spectra were obtained on a Thermo Scientific Exactive mass spectrometer.

All studies were carried out in air-saturated ethanol solutions at room temperature; methylene chloride (5%) was added to the solutions to improve the solubility of the dyad.

Quartz cells with an optical path length of l = 1 cm were used. LEDs with emitting wavelengths of 316 nm (FWHM = 11 nm) and 372 nm (FWHM = 8 nm) were used as UV light sources; the light intensity in the range of (5-9)×10^{-10} einstein cm^{-2} s^{-1} was measured by ferrioxalate actinometer. Photoisomerization quantum yields were calculated by numerical solution of a set of differential equations and averaged over several experiments (the error did not exceed 20%). All experiments with the dyad **D44B** and model compound **M1** were performed in a darkroom under red light (these compounds undergo photochemical reactions under daylight conditions).

For spectral studies, the cyclobutane **CB44B** was purified by TLC (ALUGRAM SIL, eluent: acetone-heptane 1:1).

1.3. Synthesis of dyad D44B

D44B was prepared in three steps starting from 3-methylbenzo[f]quinoline (**3MBQ**) in an overall yield of 22 %, Scheme S1. 3-{(E)-2-[4-(4-Bromo-butoxy)-phenyl]-vinyl}benzo[f]-quinoline **1**, 3-(4-methoxystyryl)benzo[f]quinoline **M**1 and methyl 2-methoxybenzoate **M2** were prepared using known procedures [S2, S3, S4].

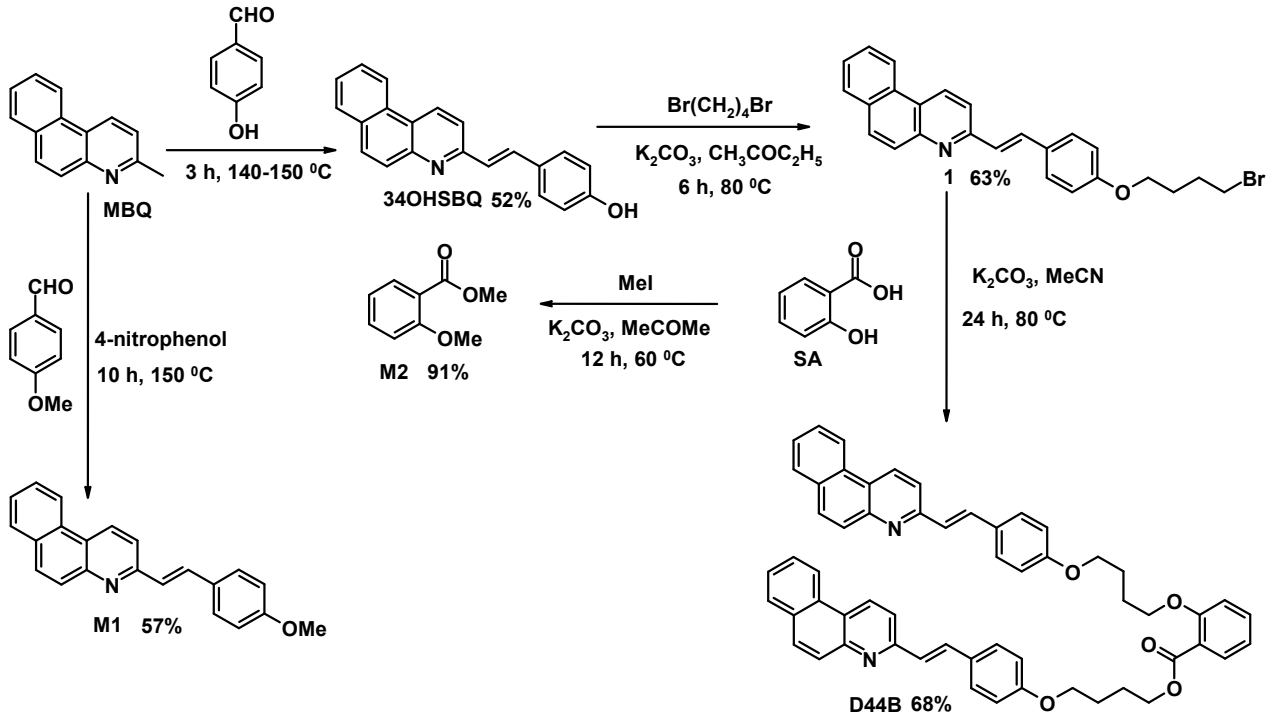

Scheme S1. Synthetic route for the dyad **D44B**, **M1** and **M2**.

2-{4-[4-((*E*)-2-Benzo[f]quinolin-3-yl-vinyl)-phenoxy]-butoxy}-benzoic acid 4-[4-((*E*)-2-benzo[f]quinolin-3-yl-vinyl)-phenoxy]-butyl ester (D44B).

A mixture of 0.036 g (0.00026 mol) of salicylic acid, 0.072 g (0.00052 mol) K_2CO_3 and 12 ml of acetonitrile was refluxed with stirring for 30 min, then added 0.257 g (0.00059 mol) of **1** and refluxed with stirring for 24 h. After cooling the precipitate was filtered off, washed first with 100 ml of water and then with 20 ml of ethyl acetate. The solid residue was recrystallized from toluene, washed with 5 ml of diethyl ether and dried at 100 °C to afford white powder of **D44B** (0.149 g, 68%); m.p. 200–202 °C. Anal. Calcd for $C_{57}H_{48}N_2O_5$. (%) C, 81.40; H, 5.75; N, 3.33. Found: C, 80.81; H, 5.61; N, 3.36; ^{1}H NMR (500 MHz, $CDCl_3$, TMS): δ 1.99 (td, 4H, , J_1 = 3.3, J_2 = 6.4, -C$\underline{H}_2$CH$_2$O); 2.03 – 2.08 (m, 4H, -C$\underline{H}_2$CH$_2$OCO); 4.01 – 4.07 (m, 4H, C$\underline{H}_2$OSBQ); 4.14 (d, 2H, J = 5.6, C$\underline{H}_2$OPh); 4.41 (d, 2H, J = 5.8, C$\underline{H}_2$OCO); 6.83 – 6.89 (m, 4H, Ph); 6.97 – 7.01 (m, 2H, Ph); 7.23 (d, 2H, J = 16.3, =CH-Ph); 7.44 – 7.48 (m, 1H, Ph); 7.49 – 7.61 (m, 10H, Ph, Ht); 7.65 (d, 2H, J = 16.3, =CH-Ht); 7.81 (dd, 1H, J_1 = 1.8, J_2 = 8.0, Ph); 7.86 – 7.90 (m, 2H, Ht); 7.91 – 7.96 (m, 4H, Ht); 8.35 – 8.39 (m, 2H, Ht); 8.61 – 8.65 (m, 2H, Ht). ^{13}C NMR (126 MHz, $CDCl_3$, RT): δ 25.64; 26.12; 26.14; 26.17; 64.61; 67.47; 67.57; 68.38; 112.96; 114.72; 114.74; 119.39; 119.40; 120.22; 120.67; 122.48; 123.91; 126.36; 126.38; 126.86; 126.98; 128.19; 128.64; 128.67; 129.33: 129.36; 129.67; 130.87; 130.93; 131.46; 131.79; 133.37; 133.64; 148.13; 155.82; 158.36; 159.43; 159.47; 166.90. IR (ν/cm^{-1}): 3051, 3030, 2944, 2927, 2915, 2903, 2867, 1691 ($\nu_{C=O}$), 1634 ($\nu_{C=C}$), 1601, 1578, 1560, 1528, 1509, 1483, 1469, 1452, 1419, 1411, 1392, 1363, 1299, 1283, 1245, 1187, 1173, 1133, 1112, 1092, 1077, 1047, 1016, 972 ($\delta_{CH=CH}$), 867, 830, 788, 744, 717, 697, 666, 636, 626, 582, 558, 540, 516, 435, 401, 385, 375.

2. NMR spectra

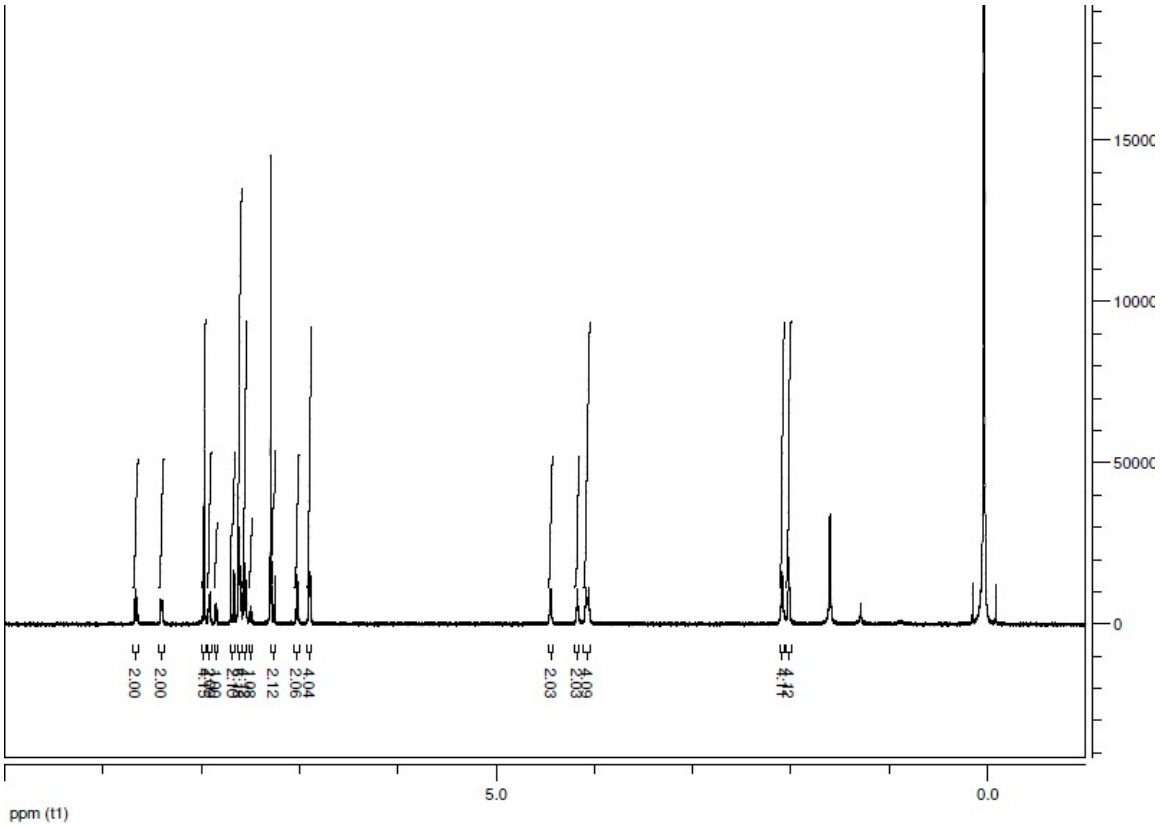

Fig. S1 ^{1}H NMR spectrum of **D44B** ($CDCl_3$).

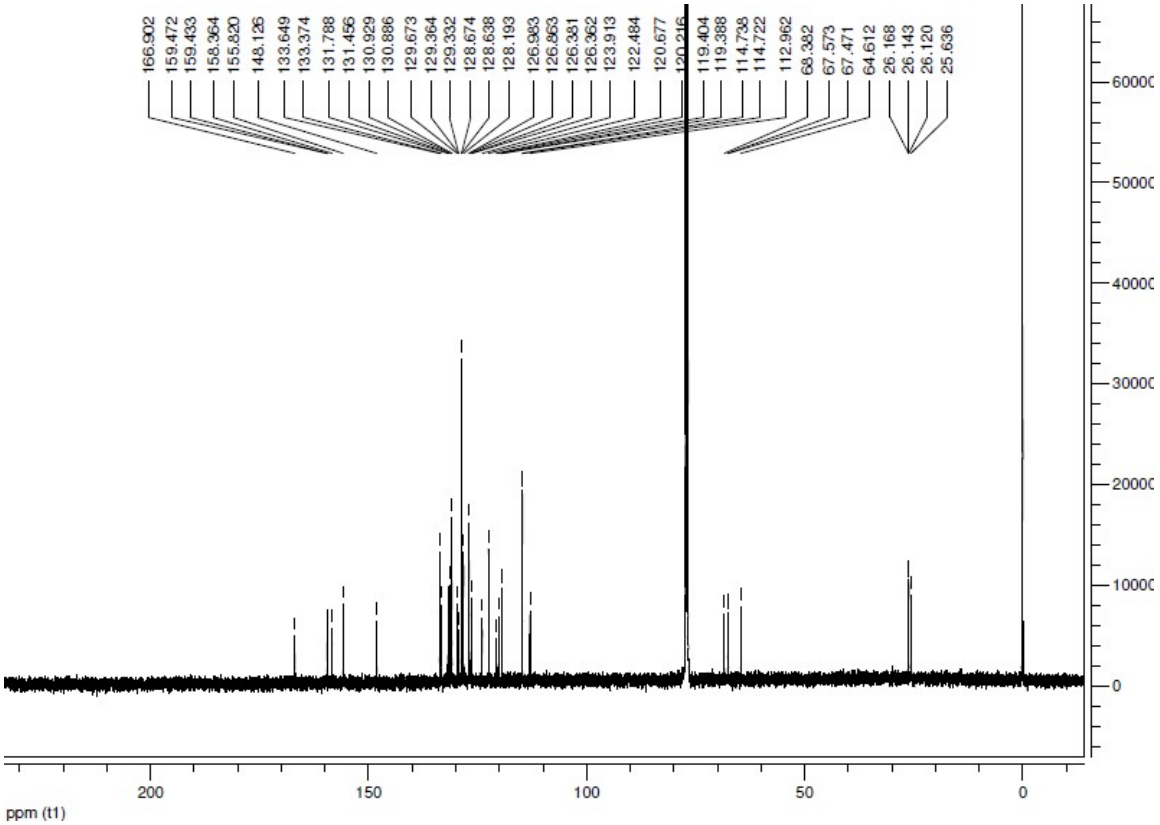

Fig. S2 ^{13}C NMR spectrum of **D44B** ($CDCl_3$)

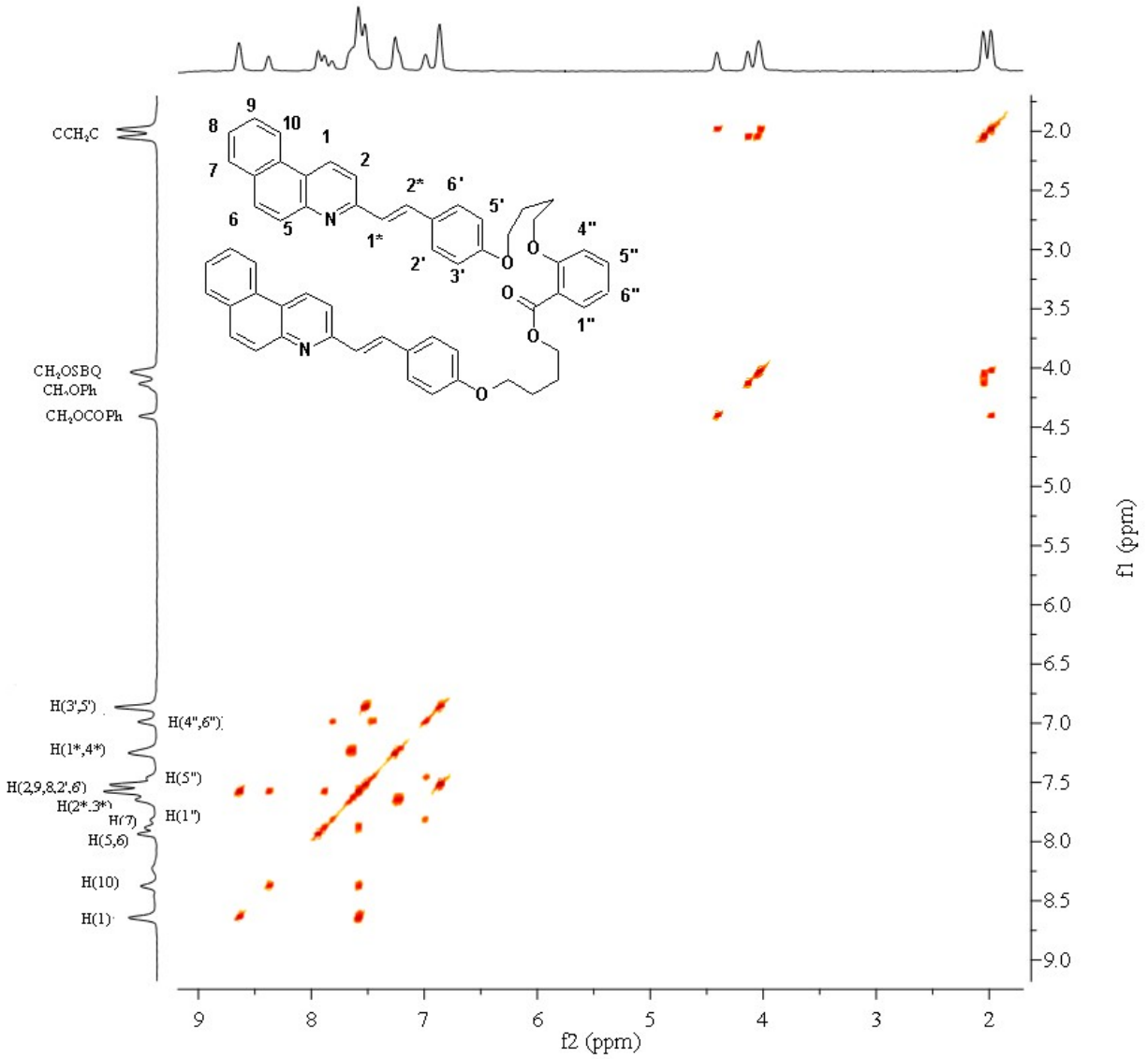

Fig. S3 Two-dimensional COSY NMR spectrum of **D44B** ($CDCl_3$).

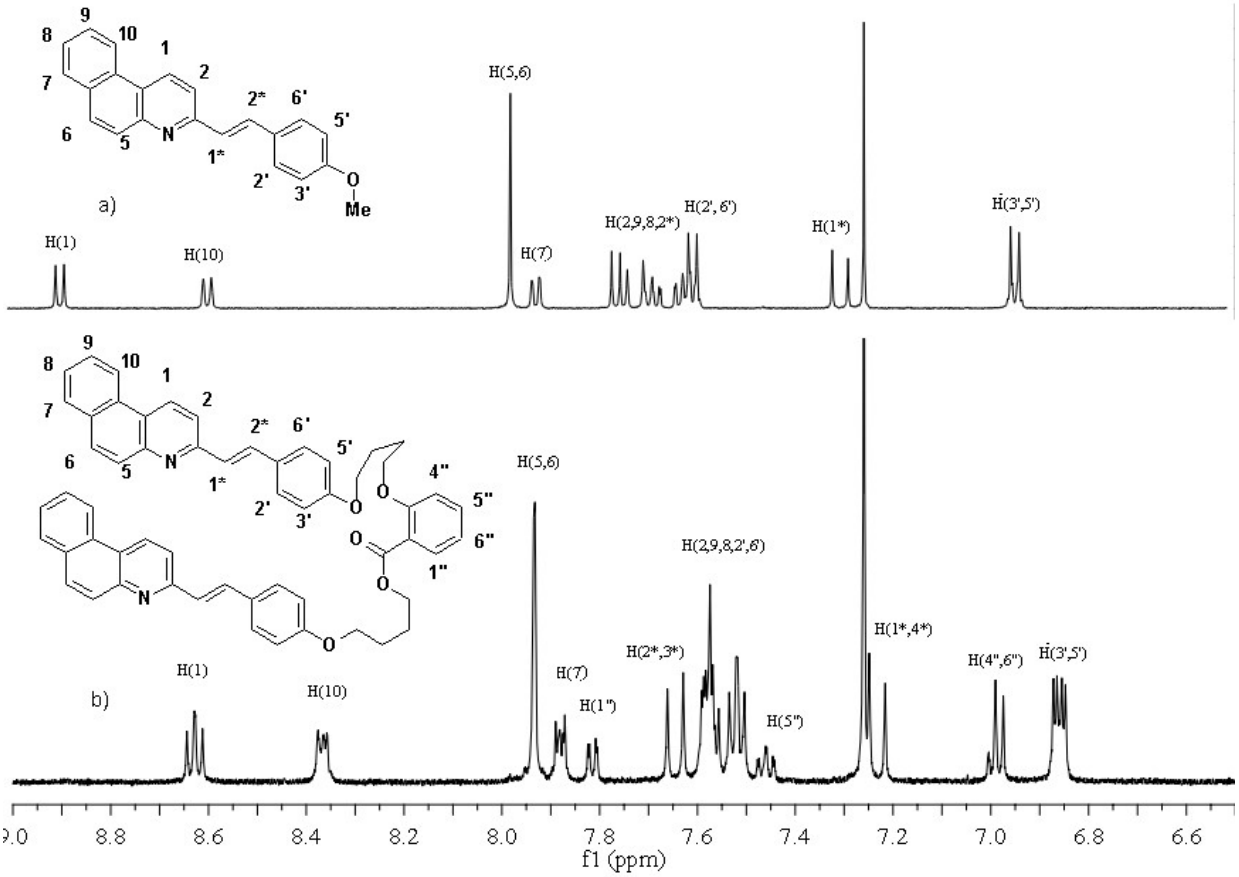

Fig. S4 Aromatic region of the ^{1}H NMR spectra (in $CDCl_3$) of (a) the model styrylbenzoquinoline **M1** and (b) dyad **D44B** (for the full spectrum see Fig. S1).

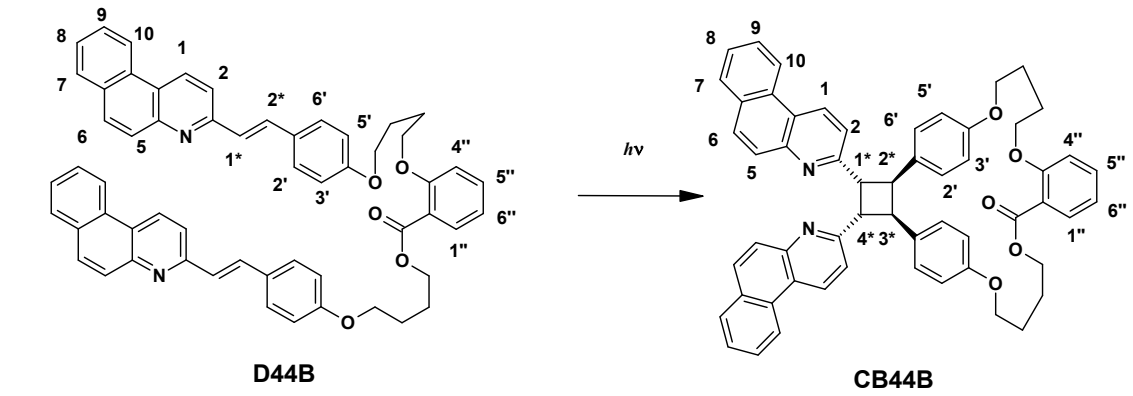

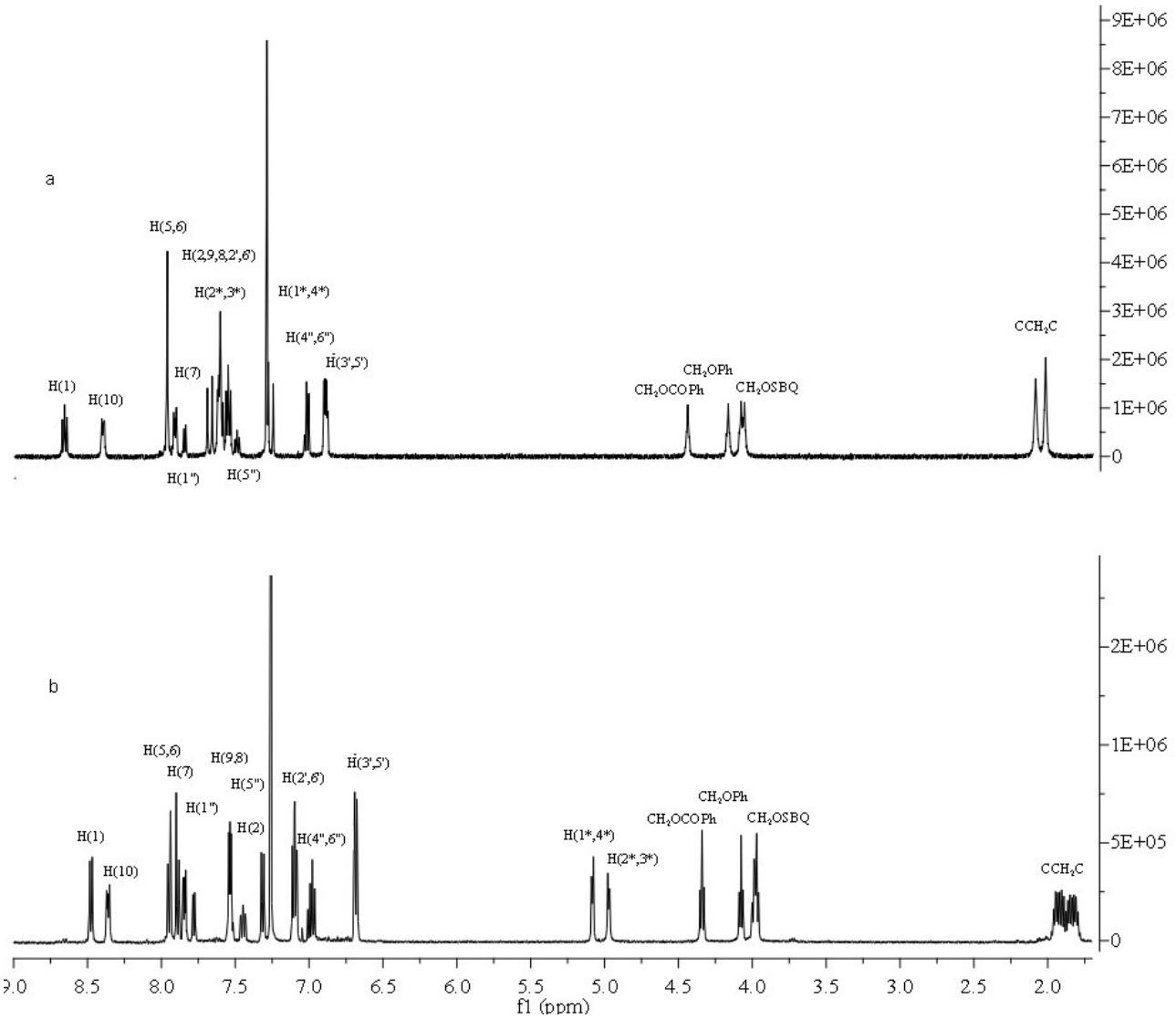

Fig. S5 ^{1}H NMR spectra of (a) **D44B** ($CDCl_3$), (b) *rctt*-**CB44B** (region of aromatic and cyclobutane ring, CH_2OCO, CH_2OSBQ, CH_2OPh groups, $CDCl_3$).

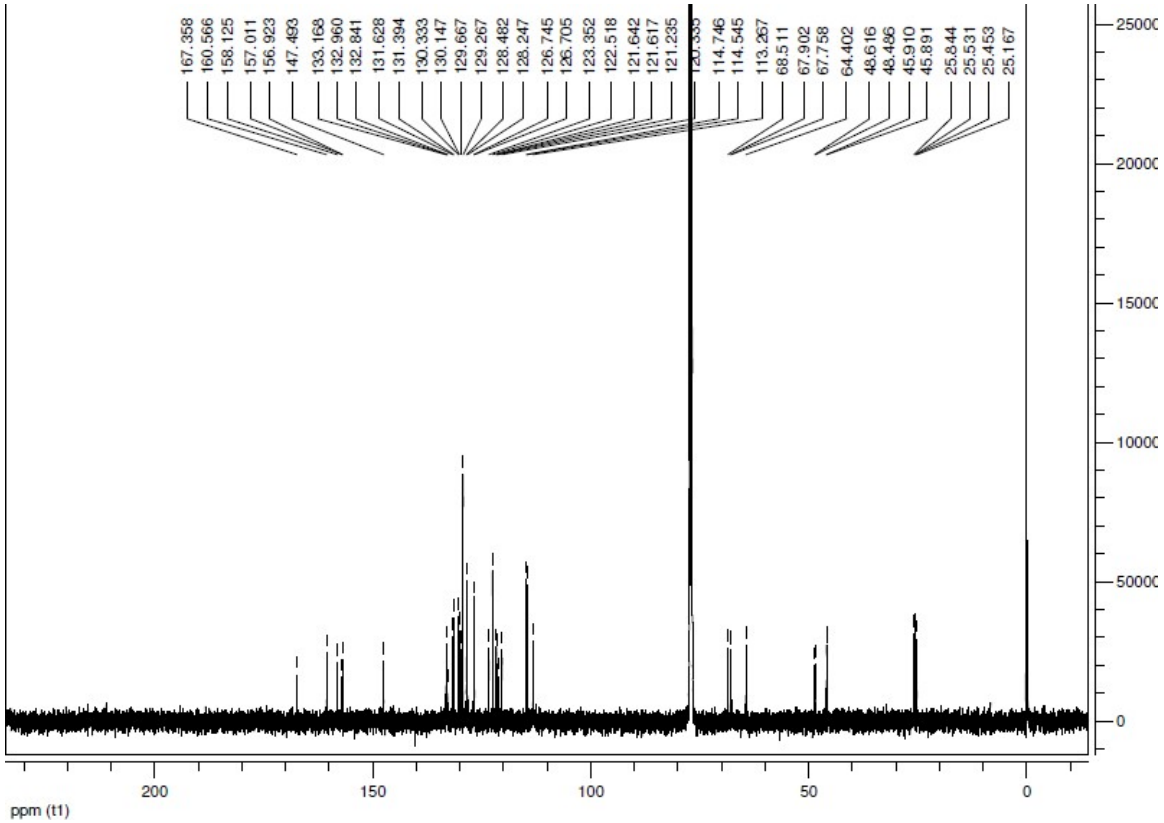

Fig. S6 ^{13}C NMR spectrum of **CB44B** ($CDCl_3$).

3. Absorption and emission spectra

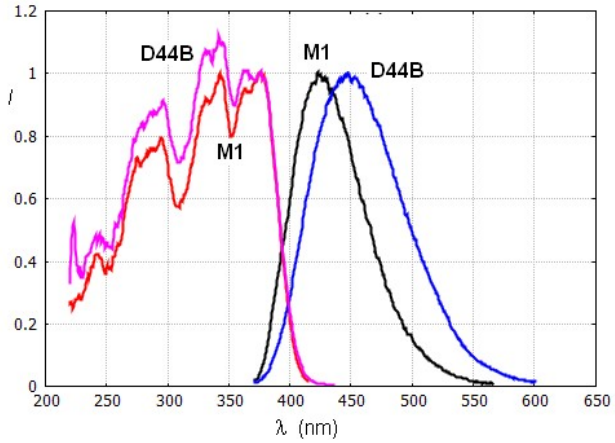

Fig. S7 Fluorescence emission (right) and fluorescence excitation (left) spectra of the dyad **D44B** and the model styrylbenzoquinoline **M1**.

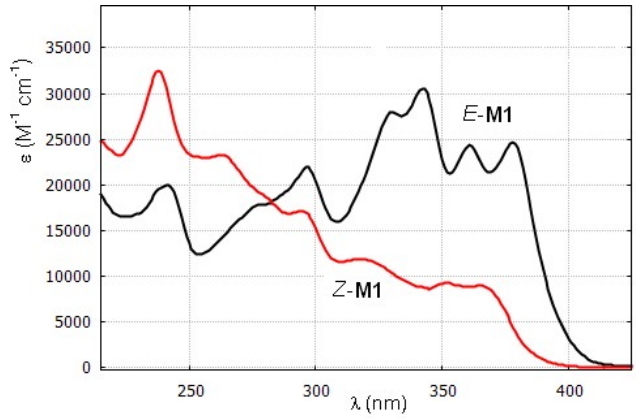

Fig. S8 Absorption spectra of the *trans*- (*E*-) and *cis*- (*Z*-) isomers of the model styrylbenzoquinoline **M1**. The spectrum of the *cis*- (*Z*-) isomer was calculated by the Fisher method based on the spectra of the *trans*- (*E*-) isomer and two photostationary states [S5].

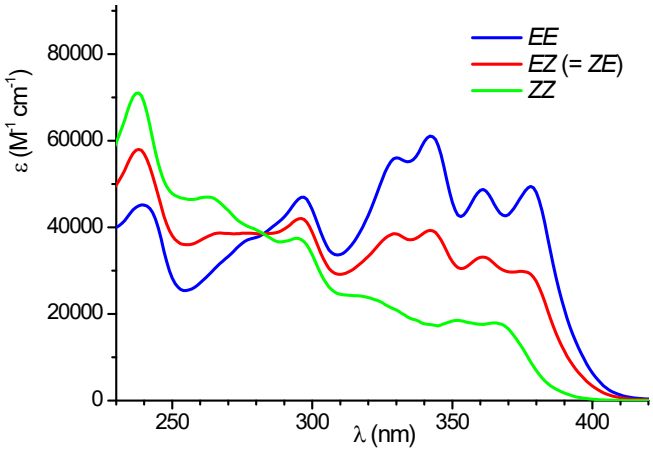

Fig. S9 Model spectra of the *EE*, *ZE*, *EZ*, and *ZZ* isomers of the dyad **D44B**, calculated as a sum of the spectra of the corresponding *trans*- (*E*) and *cis*- (*Z*) isomers of the model SBQ photochrome **M1** and methylsalicylate methyl ether **M2.**

4. Irradiation of dyad and cyclobutane with 316 nm light

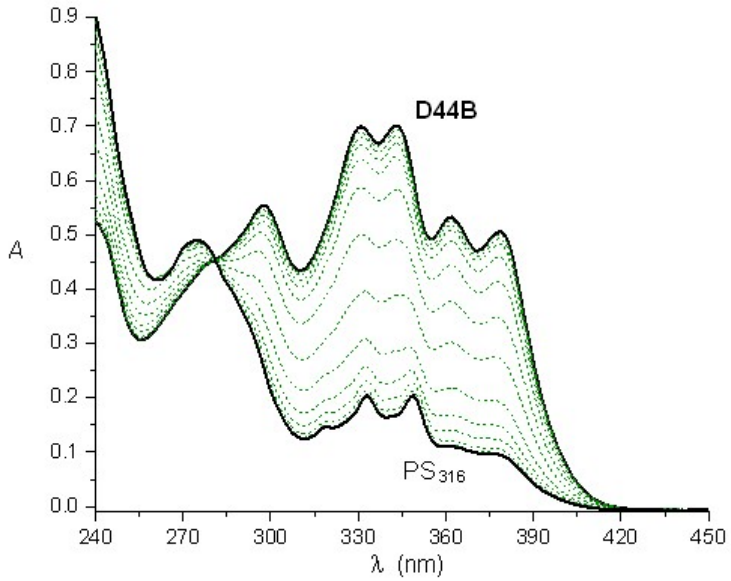

Fig. S10 Spectral changes upon irradiation of an air-saturated solution of the dyad **D44B** (1.2×10^{-5} M) with 316 nm light, intensity 1.1×10^{-10} einstein cm^{-2} s^{-1}, the total photolysis time is 10140 s.

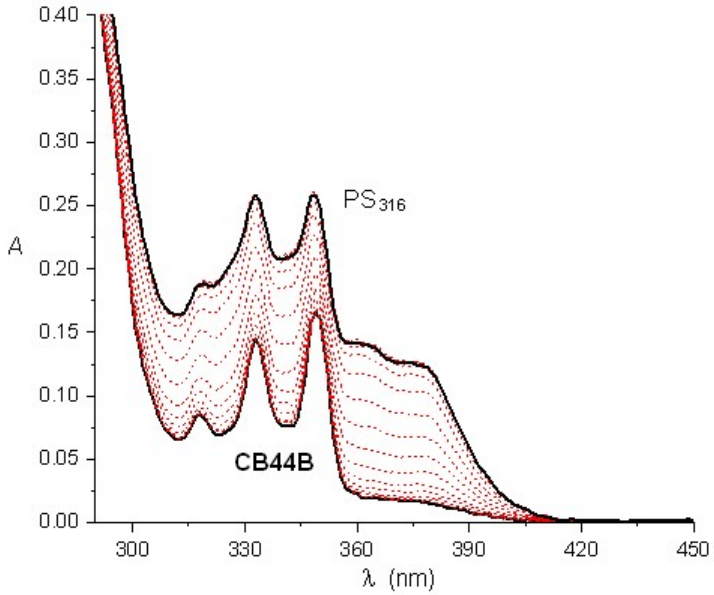

Fig. S11 Spectral changes upon irradiation of an air-saturated solution of the cyclobutane **CB44B** (1.4×10^{-5} M) with 316 nm light, intensity 1.1×10^{-10} einstein cm^{-2} s^{-1}, the total photolysis time is 20820 s.

5. Principal component analysis

The principal component analysis is one of the chemometrics methods that is used to reduce the dimensionality of large data sets, for example, the spectral data set [S6]. The experimental data consisting of a large number of measured variables, for example, the absorbance values of different samples at different wavelengths, is transformed into a smaller set containing the reduced number of variables but retaining most of the useful information from the original data. The considerable dimensionality reduction is achieved by using new formal variables, which are linear combinations of the original variables and are called principal components. Due to much less dimensionality, the reduced data set can be easily visualized in score plots. When applying to the absorption spectra analysis, the score plots allow to determine the number of independent chromophores in the reaction mixture and ascribe the observed spectral changes to a definite chemical reaction if using model spectra.

Fig. S12 reproduces Fig. 5 in the main text. The experimental spectra during photolysis of the dyad **D44B** with 316 nm and 372 nm light and the cyclobutane **CB44B** with 316 nm light are represented in the basis of the first two singular vectors. Each point on the graph corresponds to a specific spectrum of the reaction mixture during photolysis; the analysis took into account the spectral range of 230 – 420 nm with a step of 1 nm, i.e. the original matrix included 191 optical density values for each spectrum. The asterisks mark the points corresponding to the spectra of the dyad isomers, the spectra of cyclobutane **CB44B** and PS_{316}. The spectrum of the *EE* isomer was measured experimentally, the spectrum of the *EZ* isomer was calculated based on the spectra of the *trans*- and *cis*- isomers of the model SBQ photochrome **M1** and the model **M2** (see Fig. S9).

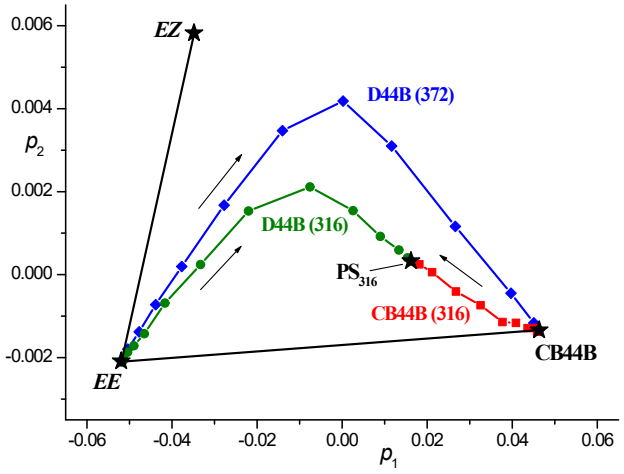

Fig. S12. Principal component analysis (score plots) of the spectral changes during photolysis of the dyad **D44B** with 316 nm and 372 nm light, the cyclobutane **CB44B** with 316 nm light, the irradiation wavelengths are shown in parentheses. The experimental spectra are given in the basis of the first two singular vectors p_1 and p_2. The asterisks mark the points corresponding to the spectra of the dyad isomers (see text), the spectra of cyclobutane **CB44B** and PS_{316}, the arrows show the direction of the spectral changes during photolysis.

Straight lines in Fig. S12 show the course of the hypothetical spectral changes during selective reactions in the dyad *EE* isomer: the *'EE–EZ'* segment characterizes only the *trans-cis* photoisomerization reaction, and the *'EE*–CB44B' segment characterizes only the photocycloaddition reaction. Upon the dyad **D44B** photolysis, experimental curves run between these segments, i.e., during the dyad photolysis, both reactions, photoisomerization and photocycloaddition, occur simultaneously. However, in the initial regions, the spectral changes are mainly due to the photoisomerization reaction. In the final regions, the spectral changes are mainly due to the photocycloaddition reaction. Under the dyad **D44B** photolysis with 316 nm light, the curve stops at the PS_{316} point, which characterizes the achievement of the photostationary states in both reactions, while under the dyad **D44B** photolysis with 372 nm light, the curve reaches the final CB44B point, characterizing the absorption of the cyclobutane **CB44B**. The reasons for this difference were discussed in the main text.

Under the dyad **D44B** photolysis with 372 nm light, the final section of the curve is straight after turning of the plot towards the CB44B point. The turning section characterizes the achievement of the quasi-PS in the photoisomerization reaction. After that, the concentration ratio of the SBQ photochromes in the form of *trans*- and *cis*- isomers in the reaction mixture ceases to change, although the total concentration of the dyad decreases due to its consumption in the photocycloaddition reaction, which is irreversible upon irradiation with 372 nm light.

NMR spectroscopy data indicate that only the *EE* isomer participates in photocycloaddition, and the only reaction product is the *rctt* cyclobutane isomer. The course of the score plot during photolysis of the cyclobutane **CB44B** with 316 nm light confirms that the cyclobutane is formed precisely from the *EE* isomer and opens into this isomer. The initial segment of this curve runs along the 'CB44B–*EE*' segment, since at the beginning of the ring-opening reaction, only the cyclobutane and the resulting *EE* isomer are present in the reaction mixture. With the accumulation of the *EE* isomer, the *trans-cis* photoisomerization reaction becomes noticeable, and the curve deviates towards the PS_{316} point and stops at this point. As above shown, the same PS_{316} point is reached upon the dyad **D44B** photolysis with 316 nm light, since the PS position does not depend on how it is reached.

[S1] H.D. Becker, Unimolecular Photochemistry of Anthracenes, *Chem. Rev*., 1993, **93**, 145-172. DOI: 0009-2665/93/0793-014.

[S2] M.F. Budyka, T.N. Gavrishova, V.M. Li, N.I. Potashova, J.A. Fedulova, Emissive and reactive excimers in a covalently-linked supramolecular multi-chromophoric system with a balanced rigid-flexible structure, *Spectrochim. Acta A. Mol. Biomol Spectrosc.*, 2022, **267**,

120565-120576. DOI: 10.1016/j.saa.2021.120565.

[S3] T.N. Gavrishova, V.M. Li, O.N. Karpov, M.F. Budyka, Synthesis and Luminescent Characteristics of 3- and 4-Hydroxy-, Carboxy-, Methoxy-, and Methoxycarbonyl-styrylbenzo[f]quinolines, *Russ. J. Org. Chem*., 2014, **50**, 1141-1144. DOI: 10.1134/S1070428014080119.

[S4] S.-T. Huang, I-J. Hsei, Ch. Chen, Synthesis and anticancer evaluation of bis(benzimidazoles), bis(benzoxazoles), and benzothiazoles, *Bioorg. Med. Chem*., 2006, **14**, 6106-6119. DOI: 10.1016/j.bmc.2006.05.007.

[S5] R. Gade, T. Porada, Determination of quantum yields and product spectra by studying reversible photoisomerizations in solution, *J. Photochem. Photobiol. A: Chem*., 1997, **107**, 27-34. DOI: 1010-6030(96)04594-7.

[S6] A.L. Pomerantsev, Chemometrics in Excel, John Wiley & Sons, Inc., Hoboken, 2014.